

Structural and luminescent characteristic of Sm³⁺ doped magnesium sulfide borate orange-red phosphor for white LED

Saddiq Abubakar Dalhatu ^{a,b,*}, Rosli Hussin ^a, Karim Deraman ^b, Ibrahim Bulus ^a, Yamusa Abdullahi Yamusa ^a, Aliyu Mohammed Aliyu ^a

^a Department of Physics, Faculty of Science, Universiti Teknologi Malaysia, 81310 Skudai, Johore Bahru, Johore, Malaysia

^b Department of Physics, Bauchi State University Nigeria, 65 Gadau, Bauchi, Nigeria

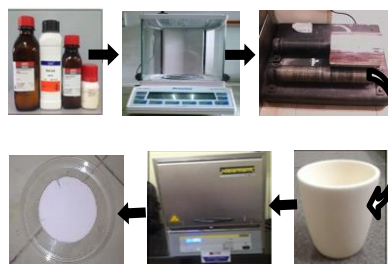
* Corresponding author: sadgambaki@yahoo.com

Article history

Received 17 May 2017

Accepted 2 October 2017

Graphical abstract



Abstract

Polycrystalline compositions based on MgO, SO₃ and B₂O₃ have both scientific and technological importance because of their useful applications. Doping with rare earth elements not only due to a rearrangement in the structure, but also to variation in the luminescence properties. Magnesium sulfide borate doped samarium oxide (MgSBO₃:Sm³⁺) phosphors were prepared by solid state reaction and their structural and luminescence characteristic were studied and reported. IR and Raman spectral studies have been made to explore the presence of functional groups and various structural units in the prepared Polycrystalline. The formation of SO₄, BO₄, BO₃, B-O-B and S-O-B structural units have been investigated. The emission and excitation properties were studied. And the results show that the emission and excitation spectra of these phosphors can be excited by ultraviolet (UV) 341, 370 and 403 nm light, and emit green, yellow and red light with intense peak at 601 nm, which are nicely in accordance with the widely applied near-UV LED chip. The emission spectral intensity of Sm³⁺ ions in the titled phosphors increases up to 1 mol% of Sm³⁺ ions and then decreases for 1.5 mol%. These results indicate that MgSBO₃:Sm³⁺ phosphor could be a potential suitable orange-red emitting phosphor candidate for white LEDs with excitation of a ~403 nm near UV LED chip.

Keywords: MgSBO₃:Sm³⁺, phosphor, luminescence, structural, orange-red LEDs, IR and raman

© 2017 Penerbit UTM Press. All rights reserved

INTRODUCTION

A light-emitting diodes (LEDs) have many significant such as energy saving, high luminous efficiency, environmental protection and maintenance when compared with the incandescent and fluorescent lamps (Kumar *et al.*, 2013). In few years, remarkable advancement can be seen in the improvement of white LED utilizing GaN and in addition InGaN chip. Obviously, three ways to produce white LEDs: (i) a blue LED is combined with a yellow YAG:Ce phosphor, (ii) mixing red, green, and blue emissions from three LEDs and (iii) exciting red/green/blue tricolour phosphors with a near-UV LED (370–410 nm) (Liao *et al.*, 2012). The third one (iii) is more convenient way to obtain white LEDs due to the advantages, generated white colour by phosphors, that is, high tolerance to UV chips' colour variation, intense luminescence efficiency as well as chemical stability. However, there exist disadvantages in this mix, viz., white emitting color changes with input power, low color rendering index due to two color mixing and low reproducibility due to strong dependence of white color quality on an amount of phosphor. To solve these problems, LED phosphors has been employing such as green, yellow and red, which are excited by ultraviolet (UV) (Mao *et al.*, 2014). However, the commercially applicable red phosphor of MgSBO₃:Eu³⁺ is lower efficient under near UV light excitation wavelength within 300 to 400 nm region, and its decomposition products are harmful to the environment (Dalhatu *et al.*, 2016). Therefore, it is an urgent to investigate new red-emitting phosphors that can be efficiently excited by the near UV LED range 350 to 410 nm chips. The rare earth are good activators, especially Sm³⁺

is an essential activator for many different inorganic lattices to yield orange-red emission due to its ⁴G_{5/2} → ⁶H_{5/2}, ⁴G₂ → ⁶H_{7/2}, ⁴G_{5/2} → ⁶H_{9/2} and ⁴G_{5/2} → ⁶H_{11/2} transitions.

Luminescent properties of phosphors are strongly dependent on the crystal structure of the host lattice and the kind of activator. To our knowledge, alkaline earth borate is considered as potential host matrices for phosphors because of its excellent thermal stabilization, stable crystal structure, cheap raw material (H₃BO₃) and excellent optical properties (Li *et al.*, 2010). The luminescence properties of samarium as a doped have been reported by many researchers. For example, LaInO₃: RE³⁺ (RE = Sm, Pr and Tb) phosphor have application for field emission displays (Liu and Lin, 2009). The Bi₂ZnB₂O₇ doped Sm³⁺ phosphor considered as a luminescence for solid state lightning (Palaspagar *et al.*, 2015). ZnGa₂O₄:Mn²⁺ and LaGaO₃:Ln³⁺ (Ln= Eu, Tb, Dy, Tm, Sm) phosphors is a candidate for applications in field of white LED (Mao *et al.*, 2014). There are some reports currently about phosphor for white LEDs (Zhang *et al.*, 2012; Li *et al.*, 2009). The IR and Raman spectroscopy are an important tool for study of structural features of a material. The borate network. Borate are known to have important properties which include low melting point, good thermal stability, good solubility of rare-earth ions (Guan *et al.*, 2013). Borate constitute an interesting system, which the network building unit can be either borate triangles (BO₃) with non-bridging atoms or borate tetrahedral (BO₄) with all bridging oxygen atoms. Borate glass can easily be melted, owning smaller mass compare to others glass network former, thermal stable and chemical durable (Dalhatu *et al.*, 2016). Previous reports show that the MgSBO₃

compound is a good type of promising host material for rare-earth ions doped phosphor. However, there are no detailed reports on the luminescence properties of $\text{MgSO}_3\text{:Sm}^{3+}$ under near UV excitation and its potential application in near UV LEDs. In this work, Sm^{3+} doped MgSO_3 was synthesized by a solid-state reaction for the first time, structural and luminescence characteristics were investigated. The results showed that $\text{MgSO}_3\text{:Sm}^{3+}$ may potentially be a good candidate as red phosphor for near UV LEDs.

EXPERIMENTAL

Materials

The starting materials were the analytic H_3BO_3 , MgO , H_2SO_4 and Sm_2O_3 (99.99% in mass), were used as beginning materials for preparing polycrystals having the compositions $10\text{MgO}\cdot 40\text{SO}_4\cdot (50-x)\text{B}_2\text{O}_3\cdot x\text{Sm}_2\text{O}_3$ mol% ($0.1 \leq x \leq 1.0$). The powder samples of $\text{MgSO}_3\text{:Sm}^{3+}$ samples were prepared by the conventional solid state reaction method. After the individual materials, had been mixed in the requisite proportions sufficiently, the powders were calcined at 800°C for 4 hours. The obtained products were $\text{MSBO}_3\text{:Sm}^{3+}$ phosphors. The structure was checked by powder X-ray diffraction (XRD) D/max-rA, $\text{CuK}\alpha$, 40 kV, 100 mA, IR measurements are carried out using Perkin-Elmer Spectrum and Raman measurement is performed by a Raman Xplora plus spectrometer. The emission and excitation spectra were measured by a Shimadzu RF-540 ultraviolet spectrophotometer. All the photoluminescence properties of the phosphors were measured at room temperature.

RESULTS AND DISCUSSION

Structure of $\text{MgSO}_3\text{:Sm}^{3+}$ phosphor

The X-ray diffraction analysis was carried out to investigate the crystalline phase of the magnesium sulfoborate doped Sm^{3+} . Fig. 1 shows the XRD pattern for MgSO_3B_3 and $\text{MgSO}_3\text{B}_3\cdot 1\text{Sm}_2\text{O}_3$ mol%. All diffraction peak positions correspond to that of the triclinic phase of MgSO_3B_3 and the diffraction peaks matched well with the standard data (JCPDS no. 01-072-1068). No Sm^{3+} ion phase was detected, proving only act as a dopant and not changing overall host lattice which confirm the formation of a single-phase MgSO_3B_3 (Dalhatu et al., 2016).

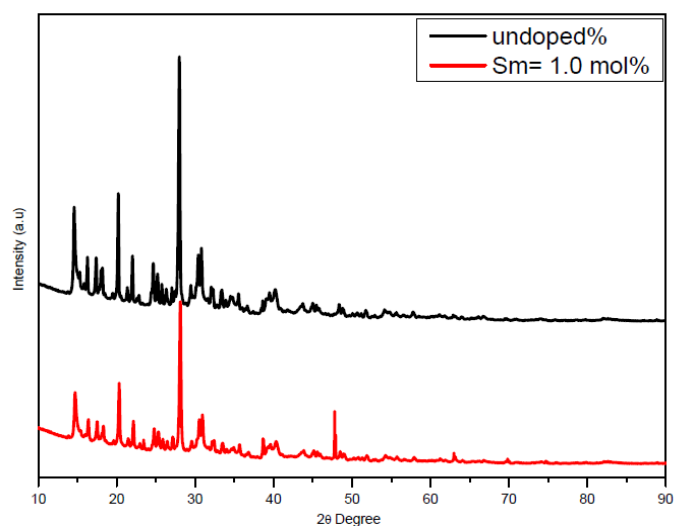


Fig. 1 XRD pattern for MgSO_3B_3 and $\text{MgSO}_3\text{B}_3\cdot 1\text{Sm}_2\text{O}_3$ mol% phosphor.

The IR spectra of $10\text{MgO}\cdot 40\text{SO}_3\cdot (50-y)\text{B}_2\text{O}_3\cdot y\text{Sm}_2\text{O}_3$ with y from 0.1 to 1.0 mol % are shown in Fig. 2. As the concentration of doped Sm^{3+} increased up to 1.0 mol %, the vibration modes are still similar without changing much in term of position and shape. The bending mode of $\delta(\text{SO}_4)^{2-}$, $(\text{BO}_3)^{-}$ is located at around $432\text{--}473\text{ cm}^{-1}$ appeared in all the spectra (Vyatchina et al., 2009). The band observed at about $548\text{--}560\text{ cm}^{-1}$ appeared in all spectra which is due to bending mode of $\delta(\text{SO}_4)$ and $\delta(\text{BO}_4)$ (Daub et al., 2013). The bending vibration

of SO_4^{2-} which is located at around $613\text{--}630\text{ cm}^{-1}$ is observed in the spectra when the content of Sm_2O_3 is from 0.3 to 1.0 mol % (Vyatchina et al., 2009). The band at around $701\text{--}715\text{ cm}^{-1}$ appeared in all spectra is due to bending of B-O-B linkages in borate network (Ganguli and Rao, 1999). The intensity of the band is increased as the content of Sm_2O_3 decreased. The vibration combination of BO_3 and BO_4 group is shifted to the high wavenumber was observed in all the spectra which is located around $870\text{--}880\text{ cm}^{-1}$ (Vyatchina et al., 2009), the intensity of the band is increased as the content of Sm_2O_3 increased. The intensity of the band is increased with increased the content of Sm^{3+} . The asymmetric stretching vibration (S-O-B) is splitting into two small bands at 924 cm^{-1} and 986 cm^{-1} (Daub et al., 2014). The splitting of the band indicates that the vibration of S-O-B is stronger with Sm_2O_3 content. The band at round $1040\text{--}1078\text{ cm}^{-1}$ appeared in all spectra which is due to B-O bond symmetric stretching vibration of the tetrahedral BO_4 units (Rada et al., 2010). Asymmetric vibration (S-O) of the SO_4 tetrahedral is located around $1204\text{--}1207\text{ cm}^{-1}$ appeared in all the spectra (Daub et al., 2013). The bands around $1340\text{--}1350\text{ cm}^{-1}$ and $1444\text{--}1447\text{ cm}^{-1}$ appeared in all spectra which is due to boroxol rings and B-O bond asymmetric stretching vibration of the trigonal BO_3 units respectively (Rada et al., 2010).

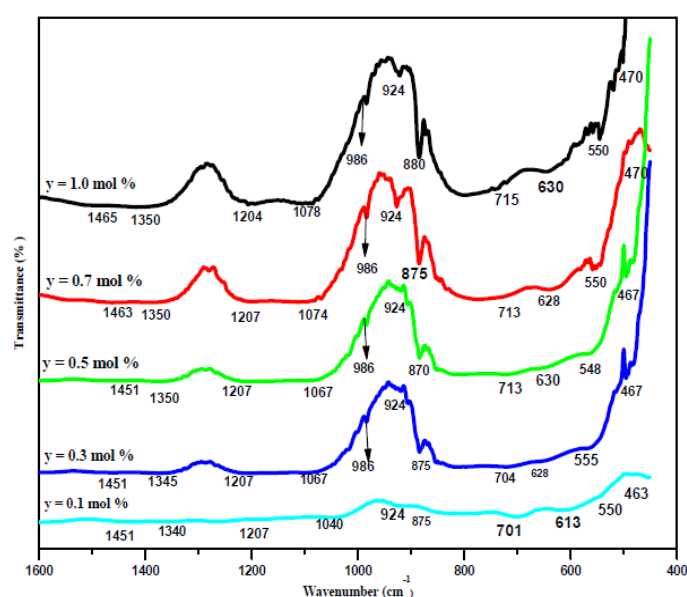


Fig. 2 IR spectra for magnesium sulfoborate doped with $0.1 \leq y \leq 1.0$ mol % of Sm^{3+} phosphor.

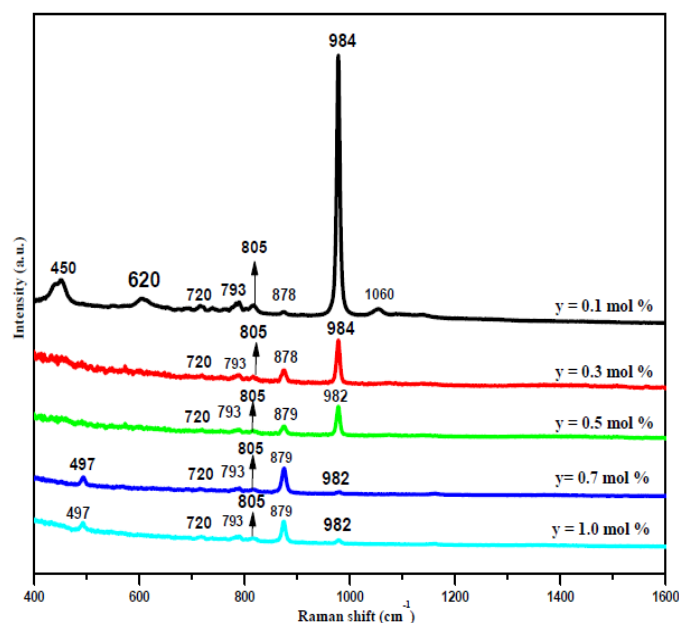


Fig. 3 Raman spectra for magnesium sulfoborate doped with $0.1 \leq y \leq 1.0$ mol % of Sm^{3+} phosphor.

The Raman spectra of $10\text{MgO}+40\text{SO}_3+(50-y)\text{B}_2\text{O}_3+y\text{Sm}_2\text{O}_3$ with $0.1 \leq y \leq 1.0$ mol % are shown in Fig. 3. The mode of SO_4^{2-} group which is around 450 cm^{-1} is observed in the Raman spectra when the content of Sm_2O_3 is 0.1 mol % (Daub et al., 2014). This is due large amount of SO_3 and small amount of B_2O_3 . While band at 497 cm^{-1} is observed in the spectra when the content of Sm_2O_3 is 0.7 and 1.0 mol % which is due to the non-ring BO_4^- (Youngman and Zwanziger, 1996). A small band at 720 cm^{-1} appeared in all the spectra which is due to bending vibrations of B-O-B linkages (Vyatchina et al., 2009). As the Sm_2O_3 content increases, one spectacular change in the Raman band is observed, i.e; the splitting of band at 804 into two small bands at 793 cm^{-1} and 805 cm^{-1} is due to symmetric vibration of boroxol rings (Yiannopoulos et al., 2001). The Raman band at 873 cm^{-1} is due to

sulfoborate type S-O-B (Ganguli and Rao, 1999). The intensity of S-O-B increased as the content of Sm_2O_3 increased. This is due to large amount of SO_3 B_2O_3 . The intense peak among all the peak was observed at band 984 cm^{-1} is due to the Symmetric stretching vibration of the SO_4 ion (Vyatchina et al., 2005). The intensity of SO_4 ion is increased as the content of Sm_2O_3 decreases with SO_3 content at 40 mol %. This shows that at small content of Sm_2O_3 the vibration of SO_4 ion is stronger. The band at 1060 cm^{-1} is observed in the spectra when content of Sm_2O_3 is 0.1 mol % which is due the mixture from vibration of BO_4 and SO_4 (Daub et al., 2014). This indicates that at large amount of boric oxide and sulfate the vibration is intense. Table 1 summarized IR and Raman band assignments and the reported values for dopants crystal samples.

Table 1 IR and Raman for magnesium sulfoborate doped Sm^{3+} phosphor.

IR	Raman	Reported values	Assignments
463–470	450–497	440-470 (Vyatchina et al., 2009)	Bending $\delta(\text{SO}_4)^{2-}$, $(\text{BO}_3)^-$.
548–555	-	500-600 (Daub et al., 2013)	bending $\delta(\text{SO}_4)$ and $\delta(\text{BO}_4)$.
613–630	620	610-630 (Vyatchina et al., 2009)	Bending $\delta(\text{SO}_4)^{2-}$
701–715	720	720-790 (Vyatchina et al., 2009)	Bending of B-O-B linkages
-	793–805	804 (Yiannopoulos et al., 2001)	boroxol rings
870–986	879–984	850-1060 (Daub et al., 2014)	Asym. stretching vibr. (S-O-B)
-	1011	1010 (Ganguli and Rao, 1999)	Symm. Stret. Vib. of SO_4^{2-}
1046–1074	1060	900-1100 (Rada et al., 2010)	Symm.stret. vibr. of BO_4 units
1204–1207	-	1200 (Daub et al., 2013)	$V_{as}(\text{S-O})$ vibration of the SO_4
1340	-	1350 (Rada et al., 2010)	boroxol rings
1451	-	1420-1550 (Rada et al., 2010)	Asymmetric stret. Vibr. of BO_3 units

Emission and excitation spectra of $\text{MgSBO}_3:\text{Sm}^{3+}$ phosphor

The excitation of $10\text{MgO}+40\text{SO}_3+(50-y)\text{B}_2\text{O}_3+y\text{Sm}_2\text{O}_3$ with $0.1 \leq y \leq 1.0$ are presented in Fig. 4. The excitation spectra are obtained by monitoring at emission wavelength of 601 nm in the range of 275-450 nm. A total of three excitation spectra were observed from ground state of $^6\text{H}_{5/2}$ to the excited state $^4\text{D}_{3/2}$ (341 nm), $^6\text{P}_{7/2}$ (370 nm) and $^6\text{F}_{7/2}$ (403 nm) of Sm^{3+} ions respectively (Liu and Lin, 2009; Zhang et al., 2006; Changmin et al., 2007). The peak position and the shape of the excitation spectra do not change as the concentration of Sm^{3+} ions increase. Meanwhile, the intensity of the excitation spectra increases as the concentration of Sm^{3+} ion increases up to 1.0 mol%, beyond is decrease in intensity with increases in concentration of Sm^{3+} ion was observed. Among the transitions, the intense excitation spectra at 403 nm ($^6\text{H}_{5/2} \rightarrow ^6\text{F}_{7/2}$) was chosen to measure the emission spectrum of $10\text{MgO}+40\text{SO}_3+(50-y)\text{B}_2\text{O}_3+y\text{Sm}_2\text{O}_3$ with $0.1 \leq y \leq 1.0$.

Fig. 5 shows the emission spectra of $10\text{MgO}+40\text{SO}_3+(50-y)\text{B}_2\text{O}_3+y\text{Sm}_2\text{O}_3$ with $0.1 \leq y \leq 1.0$. The emission spectra show four emission bands corresponding to $^4\text{G}_{5/2} \rightarrow ^6\text{H}_{5/2}$ (561 nm), $^4\text{G}_{5/2} \rightarrow ^6\text{H}_{7/2}$ (601 nm), $^4\text{G}_{5/2} \rightarrow ^6\text{H}_{9/2}$ (644 nm), and $^4\text{G}_{5/2} \rightarrow ^6\text{H}_{11/2}$ (706 nm) transition (Liao et al., 2012; Liu and Lin, 2009; Changmin et al., 2007; Xiong et al., 2014). Among the four observed bands, the $^4\text{G}_{5/2} \rightarrow ^6\text{H}_{7/2}$ is more intense. From Fig. 5, the emission spectral intensity of Sm^{3+} ions in the titled phosphors increases gradually up to 1 mol% of Sm^{3+} ions and then decreases for 1.5 mol%. This concentration quenching observed at 1mol% of Sm^{3+} ions in these phosphors may be due to nonradiative energy transfer processes among the Sm^{3+} ions (Xiong et al., 2014). These phosphors have a very distinct orange-red luminescence, which is mainly due to the luminescence of the intense $^4\text{G}_{5/2} \rightarrow ^6\text{H}_{7/2}$ (601 nm)

and $^4\text{G}_{5/2} \rightarrow ^6\text{H}_{9/2}$ (644 nm). Therefore, these transitions clearly a capable orange-red emitting phosphor for the LEDs (Palasagar et al., 2015).

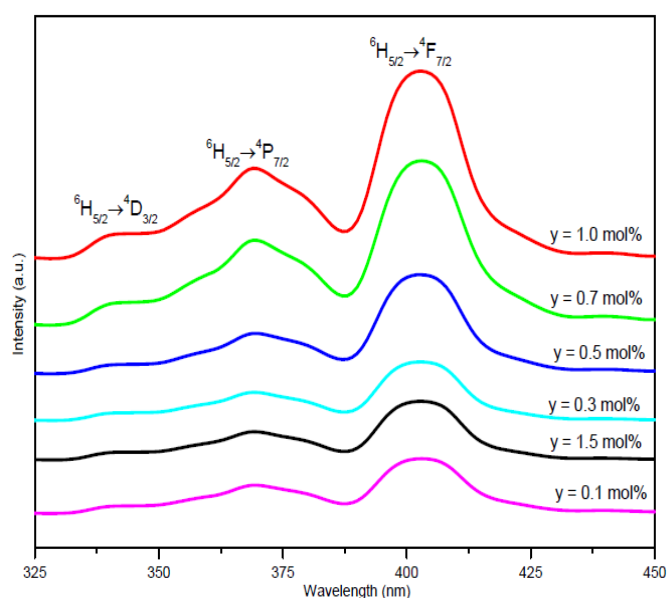


Fig. 4 Excitation spectra for magnesium sulfoborate doped with $0.1 \leq y \leq 1.5$ mol % of Sm^{3+} phosphor.

The energy level diagram of the Sm^{3+} ion doped magnesium sulfoborate phosphors are shown in Fig. 6 which shows the probable transitions involved in this process. The interaction of $\text{MgSBO}_3:\text{Sm}^{3+}$ phosphor with exciting wavelengths 403 nm, leads to the transition of Sm^{3+} ions from the ground level $^6\text{H}_{5/2}$ to the higher levels $^4\text{F}_{7/2}$. The Sm^{3+} ions from the higher states make non-radiative transition up to $^4\text{G}_{5/2}$ level after that the transitions are radiative, as the energy gap of $^4\text{G}_{5/2} \rightarrow ^6\text{H}_{5/2}$, $^4\text{G}_{5/2} \rightarrow ^6\text{H}_{7/2}$, $^4\text{G}_{5/2} \rightarrow ^6\text{H}_{9/2}$ and $^4\text{G}_{5/2} \rightarrow ^6\text{H}_{11/2}$ transitions are sufficient to give yellow-orange emission (Bedyal et al., 2014).

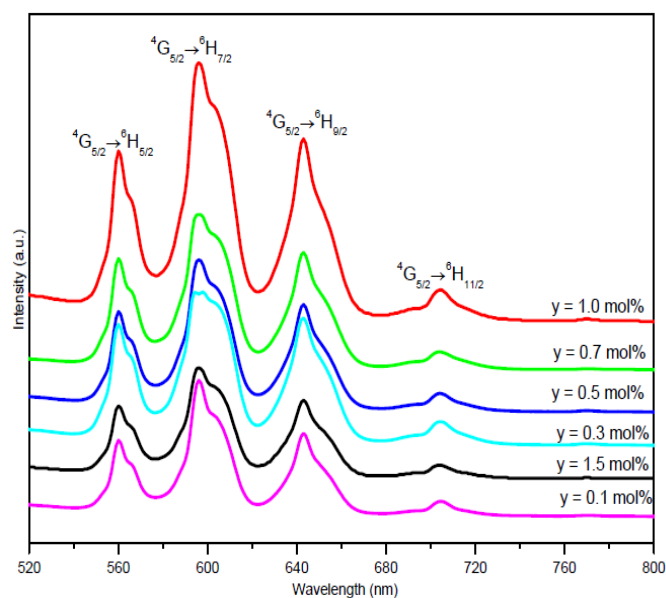


Fig. 5 Emission spectra for magnesium sulfoborate doped with $0.1 \leq y \leq 1.5$ mol % of Sm^{3+} phosphor.

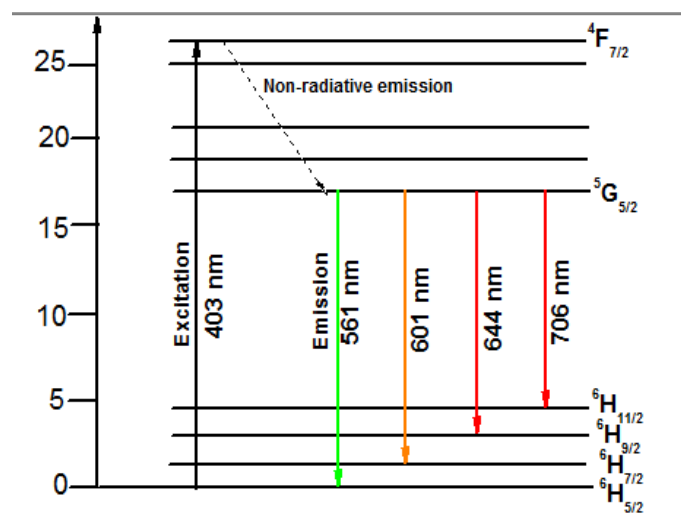


Fig. 6 The energy level diagram for magnesium sulfoborate doped with $0.1 \leq y \leq 1.5$ mol % of Sm^{3+} phosphor.

CONCLUSION

In conclusions, $\text{MgSBO}_3:\text{Sm}^{3+}$ red phosphor was prepared by solid state reaction method. XRD analysis of the prepared material shows MgSO_3B_3 phase. IR and Raman studies confirm the presence of SO_4 , BO_4 , BO_3 , B-O-B and S-O-B structural units. The excitation spectrum indicates that the phosphor can be excited by near-UV, under excitation of 403 nm, the phosphor displayed orange-red luminescence with the emission spectrum bands at 561 (green color), 601 (yellow), 644 (red color) and 706 (red color) nm which are correspond to

$^4\text{G}_{5/2} \rightarrow ^6\text{H}_{5/2}$, $^6\text{H}_{7/2}$, $^6\text{H}_{9/2}$ and $^6\text{H}_{11/2}$ transitions of Sm^{3+} , respectively. Therefore, $\text{MgSBO}_3:\text{Sm}^{3+}$ phosphors are promising phosphors for white orange-red LEDs.

ACKNOWLEDGEMENT

The authors are grateful to the Ministry of Higher Education Malaysia and UTM for providing financial assistance through the Fundamental Research Grant Scheme (FRGS), Vote number (QJ130000.2526.01H01). We thank the government of Nigeria and Bauchi State University, Gadau for a studentship (S. A. Dalhatu).

REFERENCES

- Bedyal, A. K., Kumar, V., Ntwaeaborwa, O. M. and Swart, H. C. 2014. A promising orange-red emitting nanocrystalline $\text{NaCaBO}_3:\text{Sm}^{3+}$ phosphor for solid state lighting. *Materials Research Express*, 1, 015006.
- Changmin, L., Dianlai, Y., Yingying, Z., Zhiqiang, W. and Hai, L. 2007. Photoluminescence characterization of Sm^{3+} doped fluoroborate ceramics. *Journal of Rare Earths*, 25, 143-146.
- Dalhatu, S., Hussin, R. and Deraman, K. 2016. Structural and luminescence properties of Eu^{3+} doped magnesium sulfide borate glass and crystal. *Chinese Journal of Physics*, 54(6), 877-882.
- Daub, M., Höpfe, H. A. and Hillebrecht, H. 2014. Further new borosulfates: Synthesis, crystal structure, and vibrational spectra of a $[\text{B}(\text{SO}_4)_2](a = \text{Na, K, NH}_4)$ and the crystal structures of $\text{Li}_3[\text{B}(\text{SO}_4)_4]$ and $\text{NH}_4[\text{B}(\text{S}_2\text{O}_7)_2]$. *Zeitschrift für anorganische und allgemeine Chemie*, 640(14), 2914-2921.
- Daub, M., Kazmierczak, K., Gross, P., Höpfe, H. and Hillebrecht, H. 2013. Exploring a new structure family: Alkali borosulfates $\text{Na}_3[\text{B}(\text{SO}_4)_4]$, $\text{A}_3[\text{B}(\text{SO}_4)_3](a = \text{K, Rb})$, $\text{Li}[\text{B}(\text{SO}_4)_2]$, and $\text{Li}[\text{B}(\text{S}_2\text{O}_7)_2]$. *Inorganic Chemistry*, 52(10), 6011-6020.
- Ganguli, M. and Rao, K. 1999. Studies on the effect of Li_2SO_4 on the structure of lithium borate glasses. *The Journal of Physical Chemistry B*, 103(6), 920-930.
- Guan, Y., Wei, Z., Huang, Y., Maalej, R. and Seo, H. J. 2013. $1.55\mu\text{m}$ emission and upconversion luminescence of Er^{3+} -doped strontium borate glasses. *Ceramics International*, 39(6), 7023-7027.
- Kumar, R., S., Ponnusamy, V., Jose, M. T. 2013. Synthesis and photoluminescence properties of Sm^{3+} -doped $\text{YAl}_3(\text{BO}_3)_4$ phosphor. *Luminescence*, 29(6), 649-656.
- Kumari, L., Li, W., Kulkarni, S., Wu, K., Chen, W., Wang, C., Vannoy, C. H. and Leblanc, R. M. 2010. Effect of surfactants on the structure and morphology of magnesium borate hydroxide nanowhiskers synthesized by hydrothermal route. *Nanoscale Research Letters*, 5(1), 149-157.
- Li, P., Wang, Z., Yang, Z., Guo, Q. and Li, X. 2009. Emission features of $\text{LiBaBO}_3:\text{Sm}^{3+}$ red phosphor for white LED. *Materials Letters*, 63(9), 751-753.
- Li, P., Wang, Z., Yang, Z., Guo, Q. and Li, X. 2010. Luminescent characteristics of $\text{LiCaBO}_3:\text{M}(\text{M} = \text{Eu}^{3+}, \text{Sm}^{3+}, \text{Tb}^{3+}, \text{Ce}^{3+}, \text{Dy}^{3+})$ phosphor for white LED. *Journal of Luminescence*, 130(2), 222-225.
- Mao, Z. Y., Zhu, Y. C., Wang, Y., Gan, L. 2014. $\text{Ca}_2\text{SiO}_4:\text{Ln}(\text{Ln} = \text{Ce}^{3+}, \text{Eu}^{2+}, \text{Sm}^{3+})$ tricolor emission phosphors and their application for near-UV white light-emitting diode. *Journal of Materials Science*, 49(13), 4439-4444.
- Liu, J., Li, Y., Huang, X., Li, Z., Li, G. and Zeng, H. 2007. Hydrothermal synthesis of single-crystal saibelyite $\text{MgBO}_2(\text{OH})$ nanobelt as a new host material for red-emitting rare-earth ions. *Chemistry of Materials*, 20(1), 250-257.
- Liao, J., Liu, L., You, H., Huang, H., & You, W. 2012. Hydrothermal preparation and luminescence property of $\text{MWO}_4:\text{Sm}^{3+}(\text{M} = \text{Ca, Sr, Ba})$ red phosphors. *Optik-International Journal for Light and Electron Optics*, 123(10), 901-905.
- Liu, X. and Lin, J. 2009. Synthesis and Luminescent Properties of $\text{LaInO}_3:\text{Re}^{3+}(\text{Re} = \text{Sm, Pr and Tb})$ Nanocrystalline Phosphors for Field Emission Displays. *Solid State Sciences*, 11(12), 2030-2036.
- Palasagar, R. S., Gawande, A. B., Sonekar, R. P. and Omanwar S. K. 2015. Preparation and photoluminescence properties of $\text{CaAl}_2\text{B}_2\text{O}_7:\text{Sm}^{3+}$ phosphor. *International Journal of Luminescence and Applications*, 5(1), 94-96.
- Rada, M., Rada, S., Pascuta, P. and Culea, E. 2010. Structural properties of molybdenum-lead-borate glasses. *Spectrochimica Acta Part A: Molecular and Biomolecular Spectroscopy*, 77(4), 832-837.
- Vyatchina, V., Perelyaeva, L., Zuev, M. and Baklanova, I. 2009. Structure and properties of glasses in the $\text{MgSO}_4\text{-Na}_2\text{B}_4\text{O}_7\text{-KPO}_3$ system. *Glass Physics and Chemistry*, 35(6), 580-585.

- Vyatchina, V., Perelyaeva, L., Zuev, M., Baklanova, I. and Mamoshin, V. 2005. Vibrational spectra of sulfoborate glasses. *Inorganic Materials*, 41(10), 1128-1130.
- Xiong, H., Zhu, C., Zhao, X., Wang, Z. and Lin, H. 2014. Rare earth doped lanthanum calcium borate polycrystalline red phosphors. *Advances in Materials Science and Engineering*, Article ID 819057.
- Yiannopoulos, Y., Chryssikos, G. D. and Kamitsos, E. 2001. Structure and properties of alkaline earth borate glasses. *Physics and Chemistry of Glasses*, 42(3), 164-172.
- Youngman, R. E. and Zwanziger, J. W. 1996. Network modification in potassium borate glasses: Structural studies with NMR and Raman spectroscopies. *The Journal of Physical Chemistry*, 100(41), 16720-16728.
- Zhang, X., Lu, Z., Meng, F., Lu, F., Hu, L., Xu, X. and Tang, C. 2012. A yellow-emitting $\text{Ca}_3\text{Si}_2\text{O}_7$: Eu^{2+} phosphor for white LEDs. *Materials Letters*, 66(1), 16-18.
- Wang Z., Zhang Y., Xiong Li, Li X., Guo J., Gong M. 2012. A potential red-emitting phosphor with high color-purity for near-UV light emitting diodes, *Current Applied Physics*, 12(4), 1084-1087.